Submitted to

International Europhysics Conference on High Energy Physics, EPS03, July 17-23, 2003, Aachen
(Abstract **103** Parallel Session **13**)

XXI International Symposium on Lepton and Photon Interactions, LP03, August 11-16, 2003, Fermilab

www-h1.desy.de/h1/www/publications/conf/conf_list.html

Muon Pair Production in ep collisions at HERA

H1 Collaboration

Abstract

Events containing pairs of isolated muons at high invariant masses have been measured at HERA with the H1 detector in a data sample corresponding to an integrated luminosity of 70.9 pb^{-1}. The results are compared to Standard Model predictions which are dominated by photon-photon collisions.

1 Introduction

Isolated muon pair production, $ep \longrightarrow e\mu\mu X$, at high di-muon masses has been studied by H1 using the data from 1999 and 2000. Isolated muon pairs are dominantly produced via the two-photon process, $\gamma\gamma \longrightarrow \mu^+\mu^-$, depicted in fig. 1. As well as testing QED and the photon spectrum of the proton this analysis provides constraints on backgrounds to searches for new physics. In particular, it complements the analysis of multi electron pair production where possible deviations from the standard model have been observed at large di-electron masses [1]. It is also of interest in relation to the analysis of events with a lepton and missing transverse momentum [2].

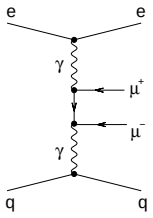

Figure 1: Muon pair production in the two-photon process (here for the deep inelastic case).

2 Selection

The muon selection is based on measurements using the central tracker and the muon detector of H1 [3]. Muon candidates are selected from charged tracks measured in the central tracker at polar angles between 20° and 160°, which are linked to tracks measured in the muon detector. For low momentum muons the finding efficiency is increased by accepting also minimal ionising particles in the Liquid Argon Calorimeter which are linked to a central track. The momentum and charge measurement is based on central tracker information. The analysis is carried out in the phase space given by a cut on the invariant mass of the muon pair ($M_{\mu,\mu} > 5$ GeV), requirements of minimal transverse momenta ($P_t^{\mu_1} > 2.0$ GeV and $P_t^{\mu_2} > 1.75$ GeV) and the given polar angle region. Background is suppressed by dedicated cuts against cosmic ray muons and an isolation requirement: the distance of the muons to the nearest track or jet in the pseudorapidity-azimuthal-plane $D^{\mu}_{Track,Jet}$ has to be greater than 1.0. For muons with high transverse momentum ($P_t^{\mu} > 10$ GeV) only $D^{\mu}_{Track,Jet} > 0.5$ is required.

3 Inclusive Isolated Muon Pair Production

Pair production of isolated muons is measured inclusively and compared to the Standard Model prediction, which is strongly dominated by electroweak production, especially by the two-photon process. Electroweak muon pair production is simulated with the GRAPE generator [4], which uses the calculation program 'GRACE' [5] to determine the Feynman amplitudes

of the corresponding diagrams in leading order. Contributions from diagrams corresponding to Bremsstrahlung with subsequent photon conversion into a muon pair and electroweak contributions like real Z^0-production with decay to $\mu^+\mu^-$ are considered in addition to the two-photon process (fig. 1). Not simulated is the negligible contribution from the Drell-Yan process in resolved photoproduction events [6]. To compare the contribution of the two-photon process to the full electroweak calculation (GRAPE), the two-photon process alone is simulated also with the LPAIR generator [7, 8]. Other sources of di-muon production have been simulated using DIFFVM [9] for the Υ-resonance, LPAIR for muons arising from $\gamma\gamma \longrightarrow \tau\tau$ and AROMA [10] for muons stemming from semi-leptonic decays in open heavy quark production ($c\bar{c}$ and $b\bar{b}$). Having corrected the data for detector effects, cross sections in the observed phase space are derived.

Fig. 2 presents the visible cross section as a function of the invariant mass of the muon pair. The mass spectrum falls steeply over more than four decades and extends up to 80 GeV. The two-photon process almost saturates the data. The shaded histograms show the expectation from the Υ and Z^0 resonances. At small masses minor contributions from open heavy flavour quark production, which are strongly suppressed due to the isolation requirement, and τ-decays are expected. The lower figures show the relative difference between data and the sum of all Standard Model contributions. The agreement between data and the standard model is very good.

The inclusive cross section as a function of the muon transverse momenta is presented in figure 3. The distribution of the transverse hadronic momentum P_t^X is depicted in fig. 4. The measured cross section is described within errors. Fig. 5 shows the cross section as a function of the invariant mass of the proton and the photon coupling to the electron and fig. 6 depicts the distribution of the missing transverse momentum. Both agree well with the prediction.

4 Elastic and Inelastic Muon Pair Production

Elastic $ep \longrightarrow e\mu\mu p$ and inelastic $ep \longrightarrow e\mu\mu X$ muon pair production are separated from each other by tagging the proton remnant X using forward detectors [11]. 92 % of the inelastic events lead to activity in either the Proton Remnant Tagger or the Forward Muon System or the forward part of the Liquid Argon Calorimeter. Fig. 7 and 8 show the resulting mass spectra for the elastic and the inelastic data samples. Elastic muon production dominates the small mass region, but both spectra extend to similar high masses and match very well with the Standard Model prediction. The error arising from the uncertainty in the separation of the two production mechanisms is conservatively estimated to be 10 %.

The total cross section of muon pair production in the observed phase space was found to be ($46.5 \pm 1.3 \pm 4.7$) pb, which agrees well with the GRAPE prediction of 46.2 pb. For inelastic di-muon production a total cross section of ($20.8 \pm 0.9 \pm 3.3$) pb was measured, which agrees within errors with the expected cross section of 21.5 pb.

5 Summary

Isolated muon pair production at high invariant masses has been analysed by H1 and both the inclusive cross section and the elastic and inelastic cross section have been found to agree very

well with the Standard Model prediction. No excess in the mass or other spectra has been observed. An increase in the integrated luminosity and extension to the μe channel will shed further light on the high mass excess reported for multi-electron production in [1].

References

[1] C. Vallée, X International Workshop on Deep Inelastic Scattering (DIS2002), Cracow.

[2] H1 Collaboration, Eur. Phys. J. C **5** (1998) 575 [arXiv:hep-ex/9806009].

[3] H1 Collaboration, Nucl. Instrum. Meth. A **386** (1997) 310.
H1 Collaboration, Nucl. Instrum. Meth. A **386** (1997) 348.

[4] T. Abe, Comput. Phys. Commun. **136** (2001) 126 [hep-ph/0012029].

[5] T. Ishikawa et.al., KEK-92-19, (1992).

[6] N. Arteaga-Romero, C. Carimalo and P. Kessler, Z. Phys. C **52** (1991) 289.

[7] S. P. Baranov, O. Dünger, H. Shooshtari and J. A. Vermaseren, *In *Hamburg 1991, Proceedings, Physics at HERA, vol. 3* 1478-1482.*

[8] J. A. Vermaseren, Nucl. Phys. B **229** (1983) 347.

[9] B. List, diploma thesis, Technische Univeristät Berlin, (H1-10/93-319) (1993).

[10] G. Ingelman, J. Rathsman and G. A. Schuler, Comput. Phys. Commun. **101** (1997) 135 [hep-ph/9605285].

[11] H1 Collaboration, [arXiv:hep-ex/0205107].

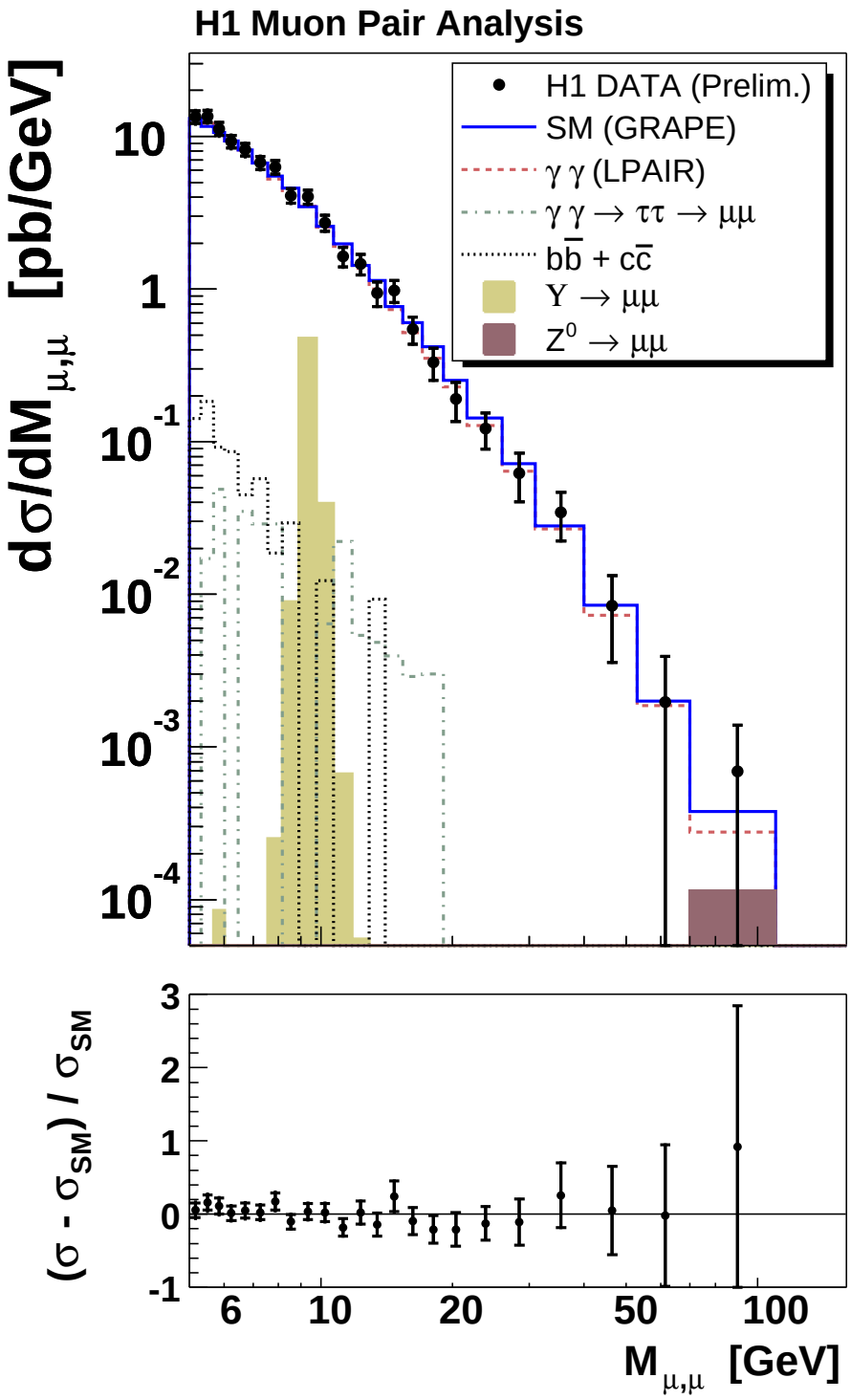

Figure 2: Invariant di-muon mass in comparison to the electroweak (EW) prediction using GRAPE. The contribution of the most important electroweak muon pair production processes are also plotted individually, i.e. the contribution from the two photon process $\gamma\gamma \rightarrow \mu\mu$ (using LPAIR) and Z^0-resonance. The contribution of additional sources of muon pair production are $\gamma\gamma \longrightarrow \tau\tau$, boson-gluon fusion ($c\bar{c}$ and $b\bar{b}$) and the decay of the Υ resonances. Also shown is the relative difference between data and all Standard Model contributions (lower figures). The inner error bars represent the statistical errors. The outer error bars represent the statistical and systematical errors added in quadrature.

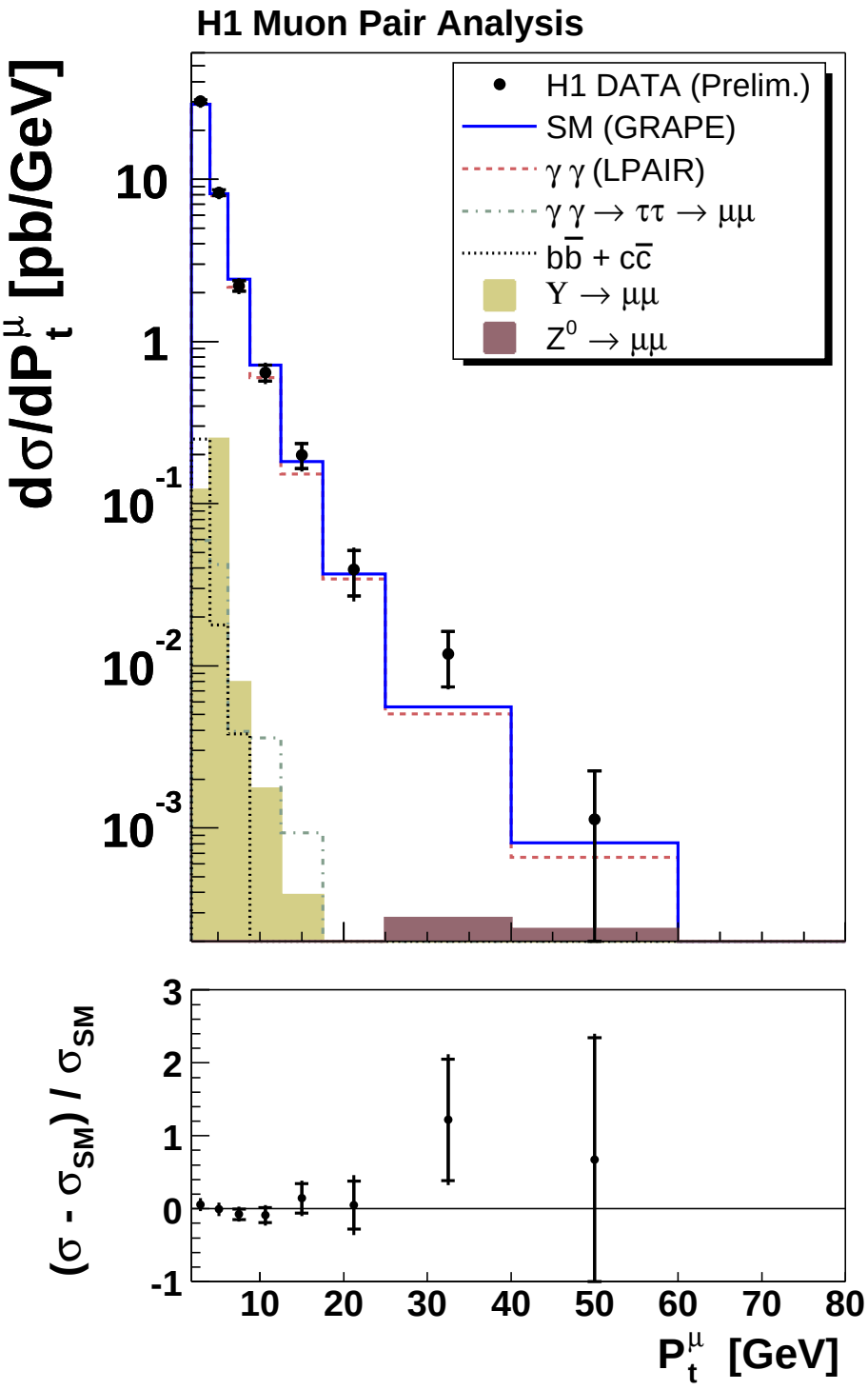

Figure 3: Cross section as a function of the muon transverse momenta (with two entries in the cross section per muon). For details see figure 2.

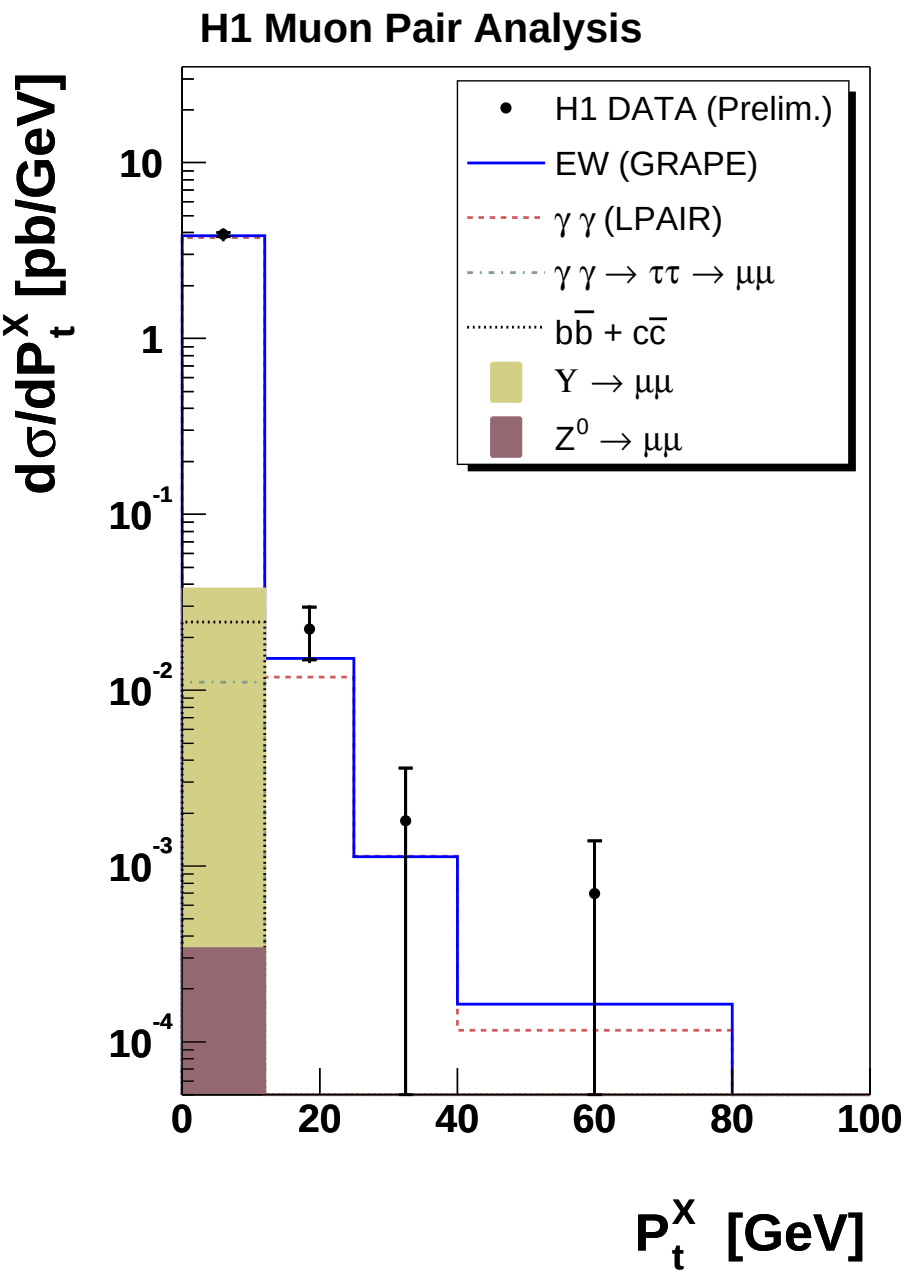

Figure 4: Cross section as a function of the hadronic transverse momentum. For details see figure 2.

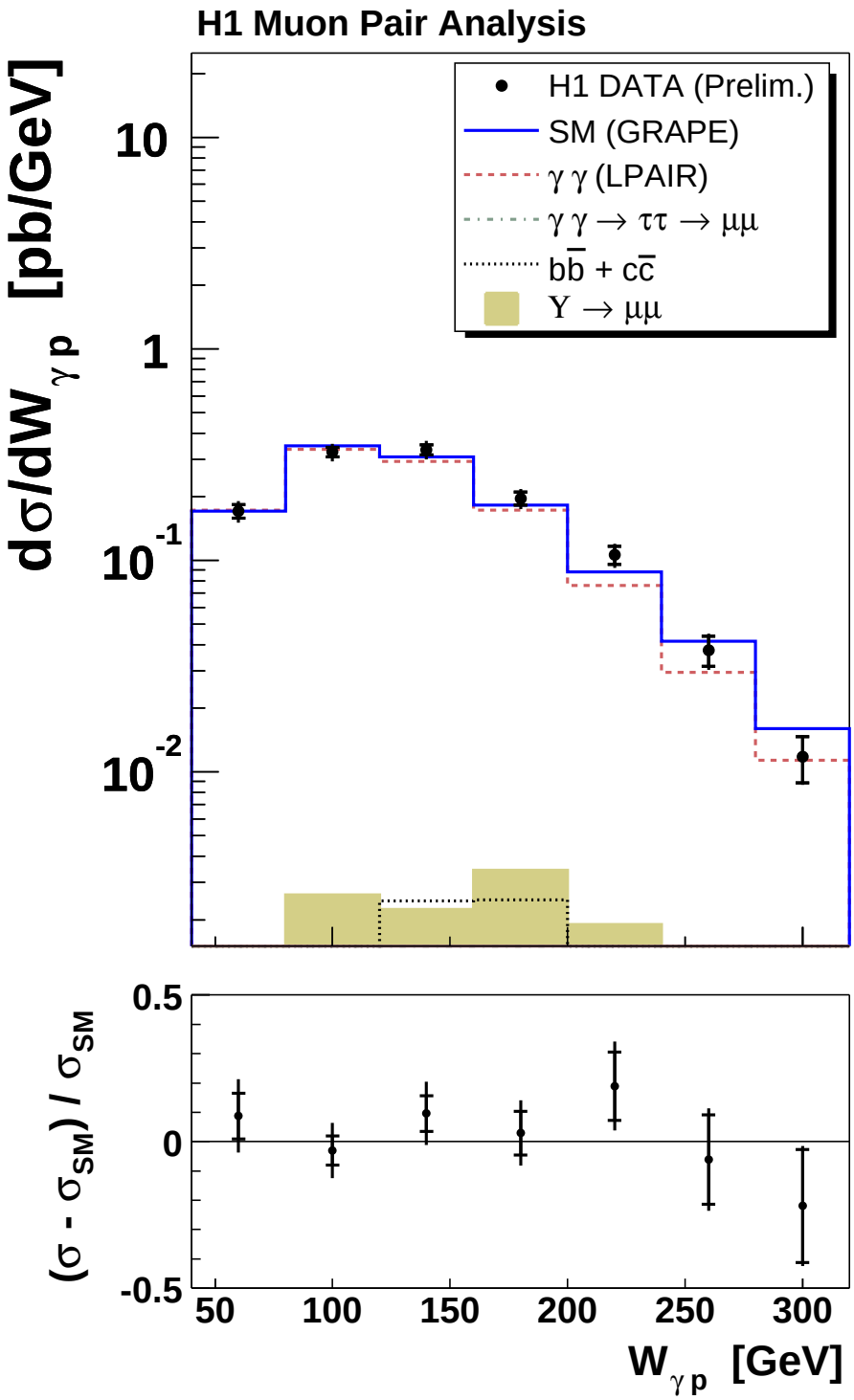

Figure 5: Cross section as a function of the invariant mass of the γ-proton system for di-muon events. For details see figure 2.

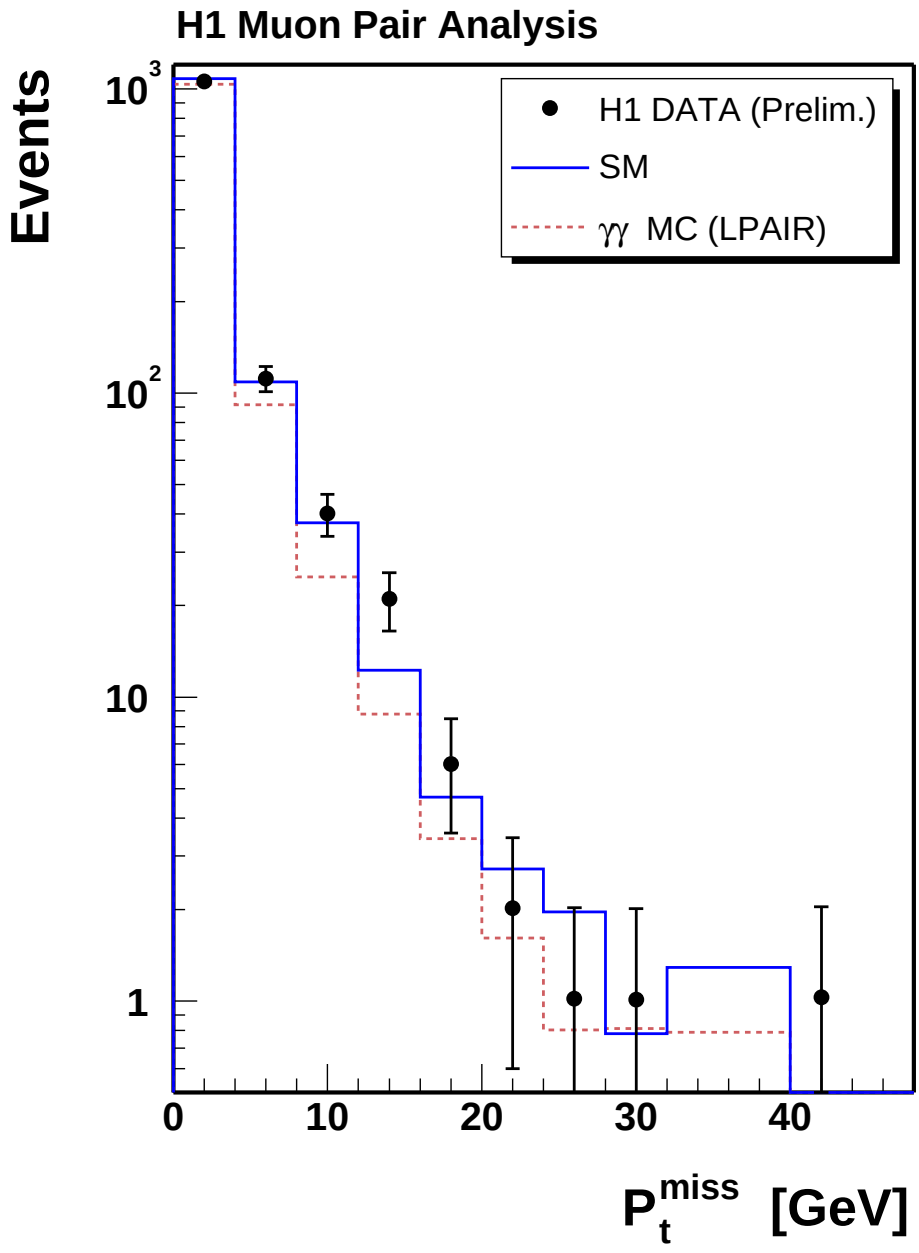

Figure 6: Distribution of the missing transverse momentum uncorrected for detector resolution. The data are compared to the full standard model expectation (SM), which is dominated by the diagrams simulated with the GRAPE Monte Carlo.

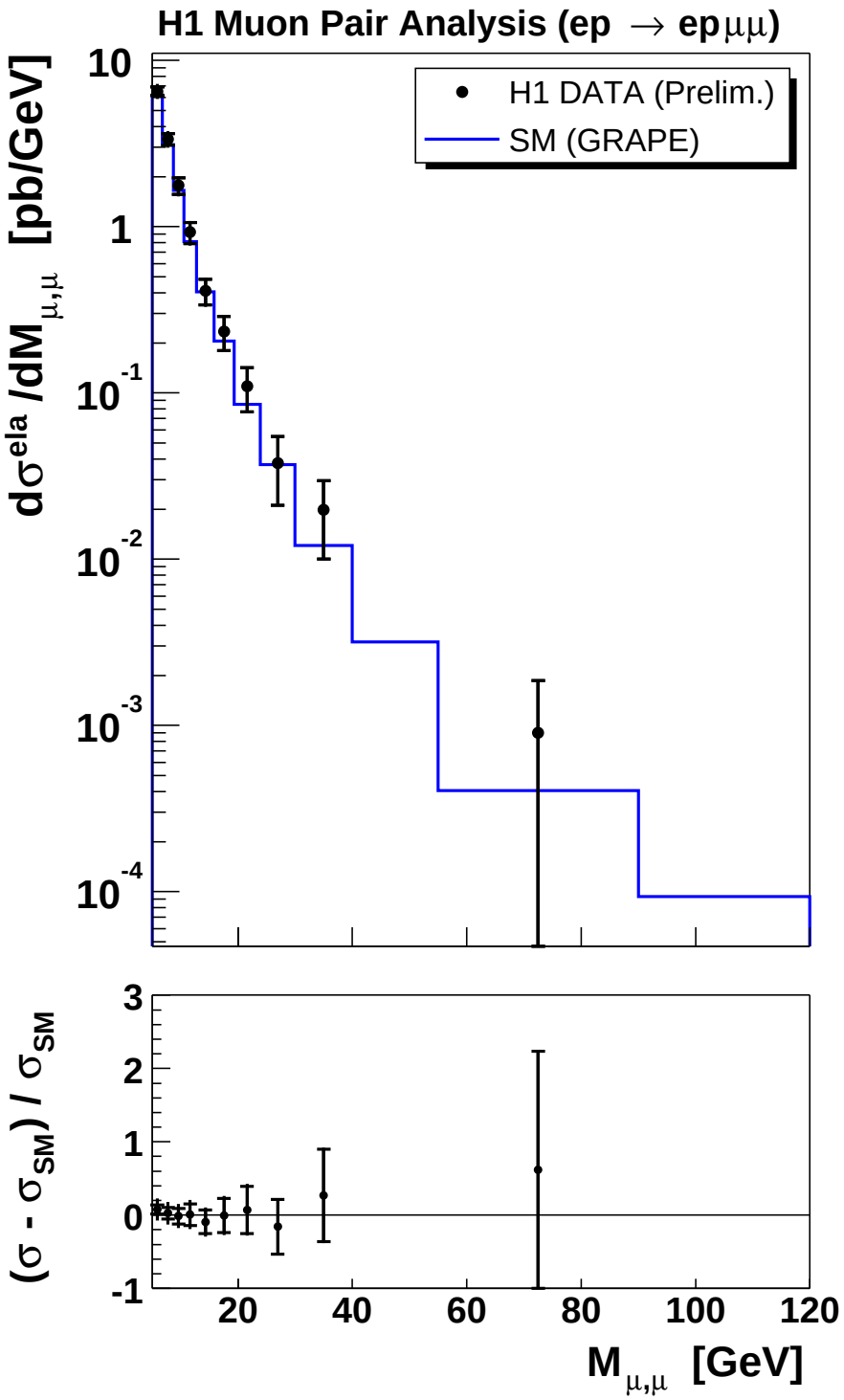

Figure 7: Cross section as a function of the invariant mass of elastically produced muon pairs.

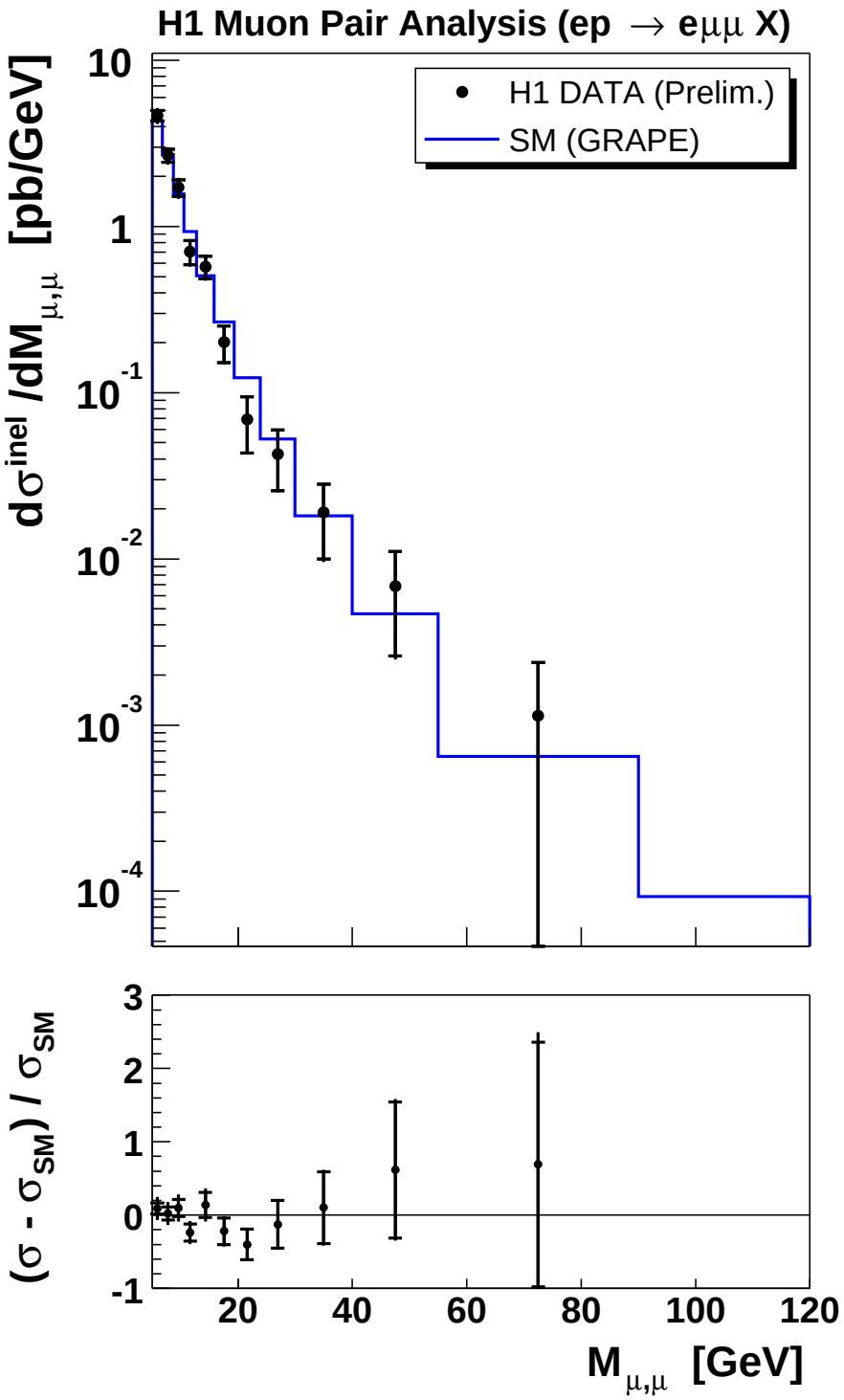

Figure 8: Cross section as a function of the invariant mass of inelastically produced muon pairs.